

# Analytic treatment of controlled reversible inhomogeneous broadening quantum memories for light using two-level atoms

J. J. Longdell\*

*Jack Dodd Centre for Quantum Technology, Department of Physics, University of Otago, Dunedin, New Zealand*

G. Hétet and P. K. Lam

*ARC COE for Quantum-Atom Optics, Australian National University, Canberra, Australian Capital Territory 0200, Australia*

M. J. Sellars

*Laser Physics Centre, RSPHysSE, Australian National University, Canberra, Australian Capital Territory 0200, Australia*

(Received 1 July 2008; published 30 September 2008)

It has recently been discovered that the optical analog of a gradient echo, in an optically thick material, could form the basis of an optical memory that is both completely efficient and noise-free. Here we present analytical calculations showing that this is the case. There is close analogy between the operation of the memory and an optical system with two beam splitters. We can use this analogy to calculate efficiencies as a function of optical depth for a number of quantum memory schemes based on controlled inhomogeneous broadening. In particular, we show that multiple switching leads to a net 100% retrieval efficiency for the optical gradient echo even in the optically thin case.

DOI: [10.1103/PhysRevA.78.032337](https://doi.org/10.1103/PhysRevA.78.032337)

PACS number(s): 42.50.Ex, 82.53.Kp, 78.90.+t

## I. INTRODUCTION

The ability to store and recall quantum states of light as coherences in atomic media is currently being actively pursued. Such quantum memories would find use in both optical-based quantum computation [1] and long-distance quantum communication [2].

Many of the current quantum memory approaches involve the use of three-level atomic systems, and store quantum information between two quasiground states [3–7]. Quantum states have been stored and recalled using this approach [3,8–10]. Three-level schemes are particularly well suited to gaseous atomic systems. Significant optical depths can be obtained using allowed transitions and long coherence times can be obtained for the ground-state coherences. Rare-earth-ion-doped solids at cryogenic temperatures have much higher atom densities and allow reasonable optical thickness to be obtained from ensembles of weak oscillators. These weak oscillators can have correspondingly long coherence times. This means that approaches involving only two-level atoms can be considered. Sangouard *et al.* [11] showed that in principle 54% efficiency can be achieved from a controlled reversible inhomogeneous broadening (CRIB) echo [5,6] with two-level atoms, in the case where the broadening mechanism is “transverse,” that is, not correlated with position along the optical path. The efficiency was limited by reabsorption; as the sample is made more optically thick, as is required to absorb the input pulse, more of the echo gets absorbed before it can make it out of the sample. Shortly afterward it was shown that the optical gradient echo or “longitudinal” CRIB echo [12], the only CRIB echo that has so far been reported experimentally, did not suffer from reabsorption problems and offered noise-free, potentially 100%

efficient storage [13]. An attractive property of these echo-based techniques is that the time-bandwidth product scales better with optical depth [2,14]. Indeed, storage and recall of multiple pulses has been demonstrated for CRIB echo memories [15] but this has proved difficult for electromagnetically induced transparency (EIT).

Following on from [13], here we present an analytic theory of the optical gradient echo (longitudinal CRIB) echo. Analytic solutions of the Maxwell-Bloch equations are derived for a pulse of light interacting with an ensemble of atoms, where the resonant frequency of the atoms varies linearly with the propagation distance. After the input pulse, the atomic coherence dephases due to the different resonant frequencies of the atomic ensemble. If the detuning of each of the atoms is reversed the ensemble rephases and produces an echo. In the case where the medium is optically thick the echo is totally efficient. We show close analogy between a gradient echo memory and a pair of beam splitters. We use this analogy to calculate the efficiency of the longitudinal echo for optically thin samples. Reversal of the inhomogeneous broadening multiple times can be easily considered using this analogy as can the operation of a number of memories placed one after the other in the beam path. Transverse inhomogeneous broadening can also be treated using the same approach. This is because transverse broadening of a collection of atoms can be modeled by a large number of optically thin longitudinally broadened collections placed one after the other. In this manner we reproduce previous results for the efficiency of transverse CRIB echoes [11] but extend the treatment to the case of multiple reversals of the broadening.

## II. THEORY

We consider the interaction of a collection of two-level atoms with a light field where a detuning of the atoms that is

\*jevon.longdell@otago.ac.nz

linearly dependent on their position can be introduced. We shall assume that the area of the incoming pulses is much less than that of a  $\pi$  pulse. This enables us to treat the atoms as harmonic oscillators. Before the detunings of the ions are flipped, the Maxwell-Bloch equations in the frame at the speed of light are [16]

$$\frac{\partial}{\partial t}\alpha(z,t) = -\left(\frac{\gamma}{2} + i\eta z\right)\alpha(z,t) + igE(z,t), \quad (1)$$

$$\frac{\partial}{\partial z}E(z,t) = iN\alpha(z,t), \quad (2)$$

where  $E$  represents the slowly varying envelope of the optical field,  $\alpha$  the polarization of the atoms,  $N$  the atomic density,  $g$  the atomic transition coupling strength,  $\gamma$  the decay rate from the excited state, and  $\eta z$  the detuning from resonance. We shall assume that the process happens fast compared to the atomic decay rate and will take  $\gamma=0$ .

In order to retrieve the light pulse, the detuning of the atoms is flipped. The Maxwell-Bloch equations describing the dynamics are the same as above except the sign of the  $i\eta z$  term in (1) is flipped, leading to (with  $\gamma=0$ )

$$\frac{\partial}{\partial t}\alpha(z,t) = +i\eta z\alpha(z,t) + igE(z,t), \quad (3)$$

$$\frac{\partial}{\partial z}E(z,t) = iN\alpha(z,t). \quad (4)$$

As mentioned above, although the treatment here is classical, the linearity of Eqs. (1)–(4) ensures that exactly the same analysis would be valid for operator-valued  $\alpha$  and  $E$ . The only added noise in the output pulses will be the vacuum noise added to preserve commutation relations in much the same way as light interacting with a beam splitter. Our results will thus hold for quantum-mechanical fields also.

The domain over which these equations will be solved is illustrated in Fig. 1. The boundary conditions are the input pulse  $E(z=-z_0,t)=f_{\text{in}}(t)$  and the initial state of the atoms. We shall assume that the atoms start in their ground state so that  $\alpha(z,t=-\infty)=0$ . By propagating forward in both  $z$  and  $t$  from these boundary conditions, one could determine the final state of the atoms and the light exiting the sample at  $z=+z_0$ . Ideally, the procedure would result in an output pulse  $E(z=+z_0,t)=f_{\text{out}}(t)$  that has the same energy and is closely related to the input pulse, and at the end of the process all the atoms would be left in their ground states,  $\alpha(z,t=+\infty)=0$ . It should be noted that we are dealing with the situation where there is no decay of the atomic states, so in order for  $\alpha(z,t=+\infty)=0$  the atoms must be left in their ground states at the end of the retrieval process; this cannot happen via decay of the atomic states.

Rather than propagating forward all the way from our boundary conditions at  $z=-z_0$  and  $t=-\infty$  to arrive at expressions for  $z=+z_0$  and  $t=+\infty$ , we will take a different approach that makes better use of the symmetry of the situation. We first solve for the behavior in region A using the boundary conditions  $\alpha(z,t=-\infty)=0$  and  $E(z=-z_0,t<0)=f_{\text{in}}(t)$ . This analysis will give us expressions for  $E$  and  $\alpha$  at the time

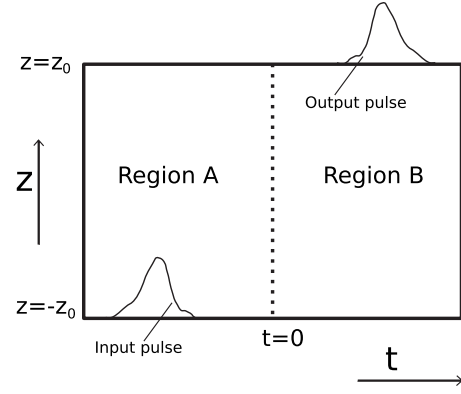


FIG. 1. The domain over which the Maxwell-Bloch equations are solved. Each horizontal slice represents one position in the sample of atoms as a function of time. The light enters the sample at  $z=-z_0$  and leaves at  $z=+z_0$ . The dotted line represents the point in time at which the detunings of the ions are flipped. In region A the dynamics are described by Eqs. (1) and (2), in region B by Eqs. (3) and (4).

when the detunings are flipped [ $\alpha(z,t=0)$  and  $E(z,t=0)$ ] as well as an expression for the light that leaves the sample before the field is flipped [ $E(z=+z_0,t<0)=f_{\text{out}}(t)$ ].

We then carry out what turns out to be a very similar analysis. Working in region B, we start with an arbitrary form output pulse [ $E(z=+z_0,t>0)=f_{\text{out}}(t)$ ] and the requirement that the atoms end up in their ground states [ $\alpha(z,t=+\infty)=0$ ] and then we work out what is needed from the other two boundary conditions  $E(z=-z_0,t>0)$  and  $(\alpha(z,t=0),E(z,t=0))$  in order for these outcomes to occur. By comparing these required boundary conditions with those that actually occur, we show that in the case of an optically thick sample the storage is completely efficient. For the case of an optically thin sample we can calculate how efficient the process will be.

The analysis of the behavior in region A is as follows. First Eq. (1) is integrated to give

$$\begin{aligned} \alpha_a(z,t) &= ig \int_{-\infty}^t dt' e^{-i\eta z(t-t')} E_a(z,t') \\ &= ig \int_{-\infty}^{\infty} dt' H(t-t') e^{-i\eta z(t-t')} E_a(z,t'); \end{aligned} \quad (5)$$

here  $H$  denotes the Heaviside step function. The above expression is in the form of a convolution, and taking the Fourier transform gives a product

$$\alpha_a(z,\omega) = igE_a(z,\omega) \left( \frac{1}{i(\omega + \eta z)} + \pi\delta(\omega + \eta z) \right), \quad (6)$$

Substituting this in Eq. (2) we get

$$\partial_z E_a(z,\omega) = -gN \left( \frac{1}{i(\omega + \eta z)} + \pi\delta(\omega + \eta z) \right) E_a(z,\omega). \quad (7)$$

Integrating this equation, we have

$$\begin{aligned}
E_a(z, \omega) &= E_a(z = -z_0, \omega) \exp \int_{-z_0}^z dz' \\
&\quad - gN \left( \frac{1}{i(\omega + \eta z')} + \pi \delta(\omega + \eta z') \right) \\
&= F_{\text{in}}^-(\omega) \exp \{ -\beta \pi [H(\omega + \eta z) - H(\omega + \eta z_0)] \} \\
&\quad \times \left| \frac{\omega + \eta z}{\omega + \eta z_0} \right|^{i\beta}, \quad (8)
\end{aligned}$$

where  $\beta = gN / \eta$ .

It can be seen that the amplitude of each spectral component is attenuated by a factor  $\exp(-\pi\beta)$  after traveling past the position in the sample where it is resonant with the atoms. It also receives a phase shift as it travels through the sample.

We make the assumption that the spectral coverage of the sample is large compared to the optical depth. That is, for each frequency of interest,  $\omega$ , in our input signal we have  $\beta\omega \ll \eta z_0$  in which case our expression for  $E_a(z, \omega)$  takes the form

$$E_a(z, \omega) = F_{\text{in}}^-(\omega) \exp[-\beta\pi H(\omega + \eta z)] \left| \frac{\omega + \eta z}{\eta z_0} \right|^{i\beta}. \quad (9)$$

Substituting  $z = +z_0$  in the above equation, one finds that the transmitted pulse is equal to the the incident pulse multiplied by an attenuation factor  $\exp(-\beta\pi)$ , i.e.,

$$f_{\text{out}}^-(t) = f_{\text{in}}^-(t) e^{-\beta\pi} \quad (10)$$

In the limit of large  $\beta$  no light is transmitted and all remains in the material during the period  $t < 0$ .

Integration of Eq. (9) with respect to  $\omega$  gives an expression for  $E_a(z, t=0)$  in the form of a convolution. Fourier transforming along the spatial coordinate, we get

$$\begin{aligned}
E_a(k, t=0) &= -f_{\text{in}}^-\left(-\frac{k}{\eta}\right) \text{sgn}(k) \beta \left| \frac{k}{\eta} \right|^{-1+i\beta} \Gamma(i\beta) \\
&\quad \times \left[ \left| \frac{k}{\eta} \right| \cosh\left(\frac{\pi\beta}{2}\right) + \frac{k}{\eta} \sinh\left(\frac{\pi\beta}{2}\right) \right]. \quad (11)
\end{aligned}$$

Here  $f_{\text{in}}(k/\eta)$  is the input field at the time  $\tau = k/\eta$  and  $\Gamma(\xi)$  is the gamma function. An expression for  $\alpha$  at the time the field was flipped can easily be obtained from the above result along with Eq. (2).

We now turn our attention to region *B* and calculate  $\alpha_b$  and  $E_b$  in that region subject to our desired boundary conditions  $\alpha_b(z, t=\infty) = 0$ ,  $E_b(z = z_0, t) = f_{\text{out}}^+(t)$ . The output field  $f_{\text{out}}^+(t)$  is at this stage undetermined.

Solution of Eq. (3) subject to the output condition  $\alpha_b(z, t=\infty) = 0$  gives

$$\begin{aligned}
\alpha_b(z, t) &= ig \int_{+\infty}^t dt' e^{i\eta z(t-t')} E_b(z, t') \\
&= -ig \int_{-\infty}^{\infty} dt' H(t' - t) e^{-i\eta z(t'-t)} E_b(z, t'). \quad (12)
\end{aligned}$$

Fourier transformation gives

$$\alpha_b(z, \omega) = -ig E_b(z, \omega) \left( \frac{i}{(\omega - \eta z)} + \pi \delta(\omega - \eta z) \right). \quad (13)$$

Substituting this in Eq. (4) and integrating, we get

$$\begin{aligned}
E_b(z, \omega) &= E_b(z = z_0, \omega) \exp \\
&\quad \times \int_{+z_0}^z dz' gN \left( \frac{i}{(\omega - \eta z')} + \pi \delta(\omega - \eta z') \right) \\
&= F_{\text{out}}^+(\omega) \exp \{ -\beta \pi [H(\omega - \eta z) \\
&\quad - H(\omega - \eta z_0)] \} \left| \frac{\omega - \eta z}{\omega - \eta z_0} \right|^{i\beta}. \quad (14)
\end{aligned}$$

In a similar manner as in region *A*, in the limit of large  $z_0$  this can be approximated as

$$E_b(z, \omega) = F_{\text{out}}^+(\omega) \exp[-\beta\pi H(\omega - \eta z)] \left| \frac{\omega - \eta z}{\eta z_0} \right|^{i\beta}. \quad (15)$$

From the above expression  $E_b(z = -z_0, t)$  can be calculated, resulting in

$$f_{\text{in}}^+(t) = f_{\text{out}}^+(t) e^{-\beta\pi}. \quad (16)$$

Also from Eq. (15) one can find an expression for  $E_b(k, t = 0)$ :

$$\begin{aligned}
E(k, t=0) &= f_{\text{out}}^+\left(-\frac{k}{\eta}\right) \text{sgn}(k) \beta \left| \frac{k}{\eta} \right|^{-1-i\beta} \Gamma(-i\beta) \\
&\quad \times \left[ \left| \frac{k}{\eta} \right| \cosh\left(\frac{\pi\beta}{2}\right) + \frac{k}{\eta} \sinh\left(\frac{\pi\beta}{2}\right) \right]. \quad (17)
\end{aligned}$$

Equations (16) and (17) give conditions that, if satisfied, will lead to a particular output pulse  $f_{\text{out}}^+(t)$  and all the atoms will be left in the ground state at the end of the process. So long as we apply an auxiliary input pulse, given by Eq. (16), a comparison of Eqs. (11) and (17) tells us that we will have an output pulse related to our input pulse by

$$f_{\text{out}}^+(t) = -f_{\text{in}}^-(t) |t|^{2i\beta} \frac{\Gamma(i\beta)}{\Gamma(-i\beta)}. \quad (18)$$

Because  $|t|^{2i\beta} \Gamma(i\beta) / \Gamma(-i\beta)$  has a modulus of 1 for all  $t$ , it can be seen that the envelope of the output pulse is a time-reversed version of the input. The practical usefulness of the memory would of course be greatly hampered by the need for this auxiliary input pulse, which must be an attenuated copy of the output pulse applied at the same time as the output pulse. However, in the situation where the sample is optically thick,  $\exp(-\beta\pi) \ll 1$ , the required input pulse is zero. To arrive at Eq. (18) one only needs to ensure that the values for  $E$  match; the values for  $\alpha$  for  $t=0$  will then also match because of Eqs. (2) and (4).

The phase between the input pulse and the output pulse changes across the pulse by  $2\beta \ln(t_{\text{end}}/t_{\text{start}})$ , where  $t_{\text{start}}$  and  $t_{\text{end}}$  are the start and end times for the output pulse. This will be a modest phase shift in most situations where the memory might be used. A value for  $\beta$  of 2 would provide sufficient optical depth for 99.999% efficiency; with this and

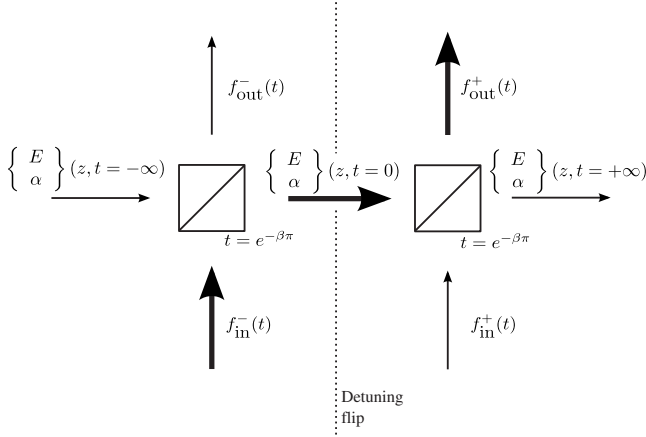


FIG. 2. Optical gradient echo memory represented as a pair of beam splitters. The bold arrows represent the flow of energy in the optically thick case. The spatial and temporal modes that correspond to each port of the beam splitter are discussed in the text.

$t_{\text{end}}/t_{\text{start}}=2$  the phase shift across the pulse would be less than  $\pi$ . This phase shift could be corrected for by some time-dependent change in the optical path length, for instance a mirror mounted on a piezo or an electro-optic phase modulator. Alternately, two memories could be used in series, with the initial frequency gradients opposite for each memory; the phase shifts of the two memories would then cancel.

**III. EFFICIENCY AND BEAM SPLITTER ANALOGS**

The fact that we can still get the desired output pulse with an optically thin sample by applying an auxiliary input pulse may not be all that helpful in the practical operation of the memory. It does, however, along with the linearity of the differential equations, enable one to determine the effect of the memory in the optically thin regime. The difference between the true output pulse when working in the optically thin regime and in the ideal case is equal to the effect of applying the auxiliary pulse alone. There is a close analogy between the operation of the memory in the finite optical depth regime and a beam splitter. An optical beam splitter takes pairs of optical modes and outputs linear combinations of these modes. The action of the memory for both times  $t < 0$  and  $t > 0$  can be reduced to that of a beam splitter, as illustrated in Fig. 2. Each of the two beam splitters has two input and two output ports. For the left-hand beam splitter the bottom input port is labeled  $f_{\text{in}}^-(t)$  and the mode of interest is the temporal mode of the optical wave packet that we wish to store. The top, output port of the left-hand beam splitter, labeled  $f_{\text{out}}^-(t)$ , represents the light that is transmitted through the sample. From Eq. (10), we can see that this transmitted light has the same temporal mode as the input light and that the amplitude transmittivity of our analog beam splitter will be  $\exp(-\beta\pi)$ . The left-hand input port and the right-hand output ports of the two beam splitters are not optical modes, but instead the beam splitter acts on, and produces, “polariton” excitations that have both an atomic and an optical component. Like the polaritons considered in

electromagnetically induced transparency [17] these are combinations of photon and atom excitations. Unlike EIT polaritons, optical gradient polaritons propagate in reciprocal space, to higher spatial frequencies, rather than traveling through the atomic medium [14].

The left-hand port of the left-hand beam splitter represents the initial state of the optical field in the sample and the atoms before the input pulse is applied for the case of our memory; during the operation of the memory this state will be a vacuum state. The right-hand output mode of the first beam splitter represents the mode of the excitation in the sample at the time the field is switched on ( $t=0$ ). The optical component of mode function is given by Eq. (11) and the atomic part can be found from Eq. (2). One explanation for why the memory works is that the output polariton mode from the left-hand beam splitter, which represents the ( $t < 0$ ) evolution, matches the input polariton mode for the right-hand beam splitter, which represents the ( $t > 0$ ) evolution.

In order to have an efficient memory we would require excitation fed into the  $f_{\text{in}}^-(t)$  port of the network, shown in Fig. 2, to be directed entirely to the  $f_{\text{out}}^-(t)$  port. This requires high reflectivity for our analog beam splitters, or, equivalently, large optical depth. The beam splitter analogy easily enables calculation of the efficiency of the echo process as a

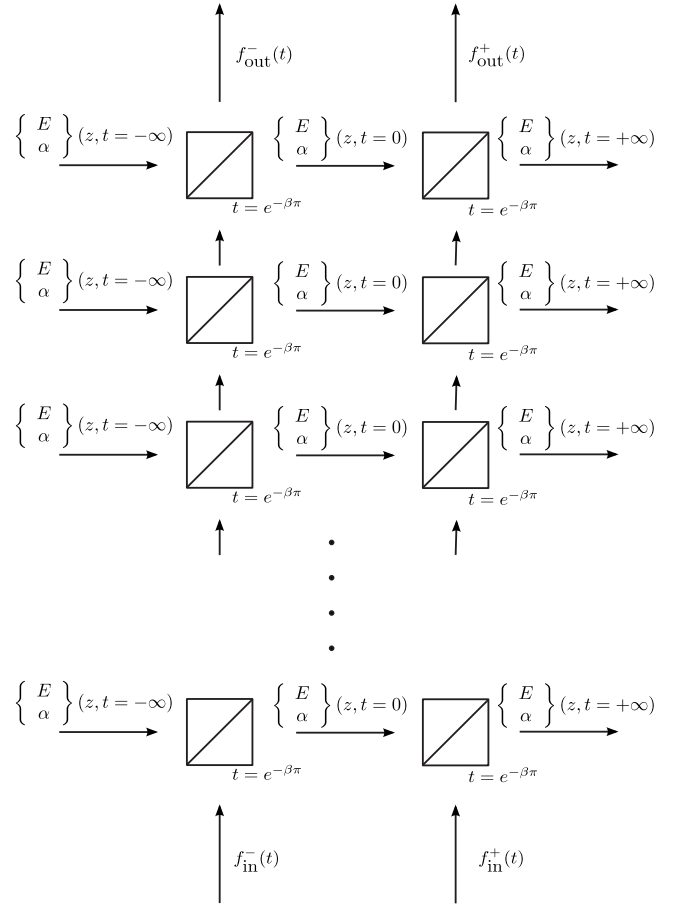


FIG. 3. Network of analog beam splitters relevant to a transverse CRIB memory modeled as a large number of optically thin gradient echo memories.

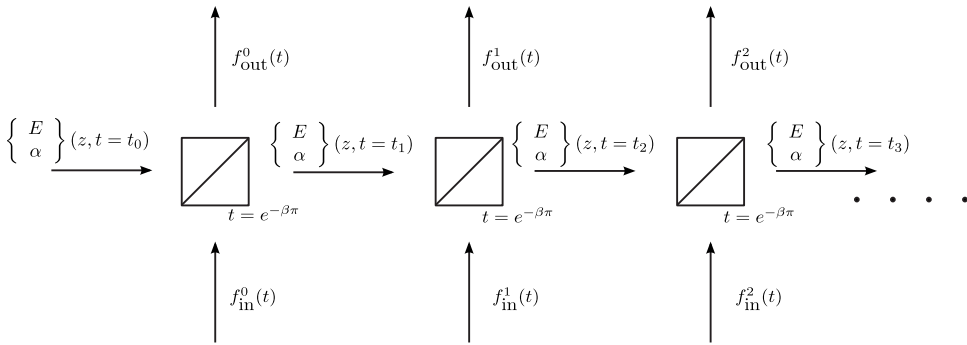


FIG. 4. Network of analog beam splitters relevant to an optical gradient echo memory where the field is switched a number of times.

function of optical depth. Because both beam splitters have an amplitude transmittivity of  $\exp(-\beta\pi)$  we end up with efficiency for the echo given by

$$(\text{Efficiency}) = [1 - \exp(-2\beta\pi)]^2.$$

This result agrees with the numerical simulations we have presented previously [13]. From the beam splitter analog one can also see immediately where the rest of the incident energy goes:  $\exp(-2\beta\pi)$  was transmitted by the sample and  $\exp(-2\beta\pi)[1 - \exp(-2\beta\pi)]$  remains in the sample.

#### IV. TRANSVERSE BROADENING AND MULTIPLE SWITCHING

Initial theoretical treatments of the efficiency of two-level controlled reversible inhomogeneous broadening echoes [11] investigated situations where the controlled detunings of the ions were not correlated with the position of the atom. Such transverse broadening would arise from a microscopic broadening mechanism. This situation can be modeled by a large number of optically thin gradient echo submemories in series. The relevant network of analog beam splitters is shown in Fig. 3. If there are  $M$  submemories, the transmitted input pulse will be attenuated by  $\exp(-2\beta\pi M)$ . There are  $M$  paths a photon can take from the input pulse  $f_{in}^-(t)$  to the output pulse  $f_{out}^+(t)$ , each of which involves two reflections and  $M - 1$  transmissions from our analog beam splitters. Because the echo from each submemory combines in phase with that from the previous memory, these paths all combine constructively to give an efficiency for the echo of  $M^2[1$

$-\exp(-2\beta\pi)]^2 \exp[-2\beta\pi(M-1)]$ . Taking the limit where each submemory is optically thin ( $\beta$  small), we arrive at an efficiency for the memory with microscopic broadening,

$$(\text{Efficiency}) = 4\beta^2 \pi^2 M^2 \exp(-2\beta\pi M) = d^2 e^{-d}.$$

Here  $d = 2\beta\pi M$  is the optical depth (the logarithm of the ratio of the energies of the incident and transmitted pulses). This result is the same as that derived in [11] by solution of the Maxwell-Bloch equations.

Another situation to which our beam splitter analogy can be applied is multiple switching of the broadening, for both longitudinal and transverse broadenings. If the broadening is switched in polarity after the first echo, the excitation remaining in the sample will again be rephased, leading to another echo. Multiple echoes of the original input pulse can be created in this way. The analog beam splitter network for multiple switching in a gradient echo is shown in Fig. 4. From this network one can see that the fraction of the input energy coming out in the  $k$ th echo is  $[1 - \exp(-2\beta\pi)]^2 \exp[-2\beta\pi(k-1)]$ . From the beam splitter network, it can be seen that with multiple switching the energy eventually leaves the sample either as a transmitted pulse or as one of the echoes. The efficiencies of the echoes as a function of  $\beta$  are plotted in Fig. 5.

The beam splitter analogy can be extended further to the case of multiple switching from a system with microscopic broadening. The network of analog beam splitters in this

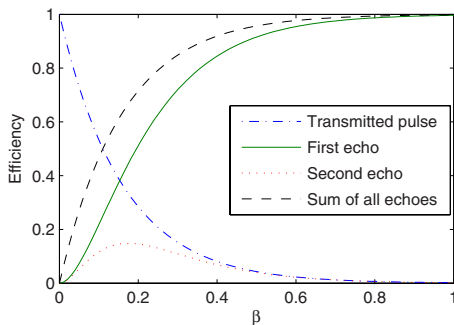


FIG. 5. (Color online) Echo efficiency for an optical gradient echo as a function of  $\beta$ , showing the effect of multiple switching. The ratio of the energies of the input and transmitted pulse is given by  $\exp(-2\pi\beta)$ .

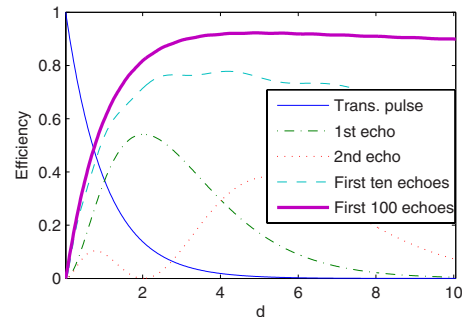


FIG. 6. (Color online) Echo efficiency as a function of optical depth for transverse broadening CRIB echo, showing the effects of multiple switching. As is shown in the figure, efficiencies significantly greater than 54% can be achieved with multiple switching, but 100% efficiency is approached relatively slowly as the number of echoes increases. Approximately 100 echoes are needed to achieve greater than 90% efficiency.

situation is similar to Fig. 3 but with a two-dimensional array of beam splitters. The amplitude of each of the multiple echoes can be calculated by summing the amplitudes of all the possible paths through the beam splitter network. This leads to the following expression for the portion of the incident energy that is output as the  $p$ th echo:

$$e_p = t^{M+p} \left| \sum_{k=1}^p \binom{p-1}{k-1} \frac{1}{k!} \left( -\frac{r^2}{t^2} \right)^k \right|^2.$$

Here  $r = 1 - \exp(-2\beta\pi)$  and  $t = \exp(-\beta\pi)$  are the amplitude transmission and reflection coefficients of the analog beam splitters. Taking the limit of a large number of optically thin memories, we get the following expression for the efficiency of the  $p$ th echo:

$$e_p = \exp(-d) \left| \sum_{k=1}^p \binom{p-1}{k-1} \frac{1}{k!} (-d)^k \right|^2,$$

where  $d$  is the optical depth. As is shown in Fig. 6, combined efficiencies significantly greater than 54% can be achieved with multiple switching.

## V. CONCLUSION

In conclusion, we have presented an analytic treatment of the optical gradient echo, or longitudinal CRIB echo. We have shown that it is completely efficient in the case of large optical depth and that recall efficiencies of 100% can also be obtained for optically thin samples by multiple switching. By modeling a system with transverse CRIB by a large number of optically thin gradients can calculate echo efficiencies in this case also, as has been shown elsewhere, the maximum echo efficiency is  $4/e^2 \approx 54\%$ . Multiple switching can improve this overall efficiency, with efficiencies of greater than 90% possible for the sum of the first 100 echoes.

## ACKNOWLEDGMENTS

J.J.L. was supported by the New Zealand Foundation for Research Science and Technology under the Contract No. NERF-UOOX0703: "Quantum Technologies." P.K.L., G.H., and M.J.S. were supported by the Australian Research Council.

- 
- [1] E. Knill, R. Laflamme, and G. J. Milburn, *Nature (London)* **409**, 46 (2001).
  - [2] C. Simon, H. de Riedmatten, M. Afzelius, N. Sangouard, H. Zbinden, and N. Gisin, *Phys. Rev. Lett.* **98**, 190503 (2007).
  - [3] B. Julsgaard, J. Sherson, J. I. Cirac, J. Fiurasek, and E. S. Polzik, *Nature (London)* **432**, 482 (2004).
  - [4] M. Fleischhauer and M. D. Lukin, *Phys. Rev. A* **65**, 022314 (2002).
  - [5] S. A. Moiseev and S. Kröll, *Phys. Rev. Lett.* **87**, 173601 (2001).
  - [6] B. Kraus, W. Tittel, N. Gisin, M. Nilsson, S. Kröll, and J. I. Cirac, *Phys. Rev. A* **73**, 020302(R) (2006).
  - [7] A. V. Gorshkov, A. André, M. D. Lukin, and A. S. Sørensen, *Phys. Rev. A* **76**, 033806 (2007).
  - [8] T. Chanelière, D. N. Matsukevich, S. D. Jenkins, S.-Y. Lan, T. A. B. Kennedy, and A. Kuzmich, *Nature (London)* **428**, 833 (2005).
  - [9] M. D. Eisaman, A. André, F. Massou, M. Fleischhauer, A. S. Zibrov, and M. D. Lukin, *Nature (London)* **438**, 837 (2005).
  - [10] J. Appel, E. Figueroa, D. Korystov, M. Lobino, and A. I. Lvovsky, *Phys. Rev. Lett.* **100**, 093602 (2008).
  - [11] N. Sangouard, C. Simon, M. Afzelius, and N. Gisin, *Phys. Rev. A* **75**, 032327 (2007).
  - [12] A. L. Alexander, J. J. Longdell, M. J. Sellars, and N. B. Manson, *Phys. Rev. Lett.* **96**, 043602 (2006).
  - [13] G. Hétet, J. J. Longdell, A. L. Alexander, P. K. Lam, and M. J. Sellars, *Phys. Rev. Lett.* **100**, 023601 (2008).
  - [14] G. Hétet, J. J. Longdell, M. J. Sellars, P. K. Lam, and B. C. Buchler, e-print arXiv:0801.3860.
  - [15] A. L. Alexander, J. J. Longdell, M. J. Sellars, and N. B. Manson, *J. Lumin.* **127**, 94 (2007).
  - [16] M. D. Crisp, *Phys. Rev. A* **1**, 1604 (1970).
  - [17] M. Fleischhauer and M. D. Lukin, *Phys. Rev. Lett.* **84**, 5094 (2000).